UC Irvine
UC Irvine Previously Published Works

Title

Unfolding of pyridoxal 5′-phosphate-dependent O-acetylserine sulfhydrylase probed by time-resolved tryptophan fluorescence

Permalink

https://escholarship.org/uc/item/0fj5t2q5

Journal

Biochimica et Biophysica Acta, 1596(1)

ISSN

0006-3002

Authors

Bettati, Stefano
Campanini, Barbara
Vaccari, Simona
et al.

Publication Date

2002-04-01

DOI

10.1016/s0167-4838(01)00316-8

Copyright Information

Peer reviewed

Unfolding of pyridoxal 5′-phosphate-dependent *O*-acetylserine sulfhydrylase probed by time-resolved tryptophan fluorescence

Stefano Bettati [a,b,c,]*, Barbara Campanini [b,c], Simona Vaccari [b], Andrea Mozzarelli [b,c], Giulio Schianchi [a,c], Theodore L. Hazlett [d], Enrico Gratton [d], Sara Benci [a,c]

[a] *Institute of Physical Sciences, University of Parma, Via Volturno 39, 43100 Parma, Italy*
[b] *Department of Biochemistry and Molecular Biology, University of Parma, 43100 Parma, Italy*
[c] *National Institute for the Physics of Matter, University of Parma, 43100 Parma, Italy*
[d] *Laboratory of Fluorescence Dynamics, University of Illinois at Urbana-Champaign, Urbana, IL 61801, USA*

Abstract

Proteins utilizing pyridoxal 5′-phosphate as a coenzyme constitute a large superfamily and are currently classified into three functional groups and five structural fold types. Despite the variability of sequences and catalyzed reactions, they share relevant structural, dynamic and functional properties. Therefore, they constitute an optimal system to investigate the relative influence of primary sequence and coenzyme interactions on folding pathways, structural stability and enzymatic function. *O*-Acetylserine sulfhydrylase is a dimeric pyridoxal 5′-phosphate dependent enzyme that catalyzes the synthesis of L-cysteine from *O*-acetylserine and sulfide. The time-resolved fluorescence study of *O*-acetylserine sulfhydrylase unfolding, here reported, indicates that the coenzyme stabilizes the protein structure. The dependence on denaturant concentration of tryptophan lifetimes in the holo- and apo-enzyme demonstrates that the interactions with the coenzyme stabilize the C-terminal domain to a higher extent with respect to the N-terminal domain. This result is discussed in terms of a linkage between the differential stabilization brought about by the coenzyme and the different degrees of conformational flexibility required by the specialized functional role of distinct protein regions. © 2001 Elsevier Science B.V. All rights reserved.

Keywords: Enzyme; Unfolding; Energy transfer; Tryptophan; Time-resolved fluorescence; Pyridoxal 5′-phosphate

1. Introduction

O-Acetylserine sulfhydrylase (OASS) is a homodimeric enzyme (34 450 Da/protomer for the *Salmo-* *nella typhimurium* enzyme) catalyzing the last step of cysteine biosynthesis in bacteria and plants. The three-dimensional structure of OASS from *S. typhimurium* (EC 4.2.99.8) has been determined both in the absence [1] and presence of ligands [2] and anions [3]. Microspectrophotometric studies [4] endorsed the functional validity of the specific structural conformations by assessing the catalytic competence of the enzyme in the crystalline form. In the absence of ligands, the coenzyme pyridoxal 5′-phosphate (PLP) is bound via a Schiff base to the side chain of Lys41 [5], at the interface between the two

---

domains constituting each subunit of the dimer [1] (Fig. 1). The absorption, fluorescence and phosphorescence properties of PLP and tryptophan residues have been exploited to investigate the conformational properties, dynamics and reaction mechanism of OASS [6–11]. Large conformational changes upon ligand binding have been detected with spectroscopic [7,9] and crystallographic methods [2]. The location of the two tryptophan residues, belonging to helical regions of the N-terminal (Trp50) and C-terminal domains (Trp161) (Fig. 1) allows one to probe the conformational state of separate regions of the protein during catalysis [11] and unfolding [12]. The extent of the energy transfer occurring from Trp50 to PLP [8,11], being sensitive to the donor–acceptor relative distance and transition dipoles orientation, provides a supplemental probe of structural dynamics.

PLP-dependent enzymes catalyze a variety of reactions mainly related to amino acid metabolism. The members of this large superfamily, widely spread among living organisms, are organized into three functional groups, the α, β and γ families, based on the chemical characteristics of the catalyzed reactions [13]. On the basis of sequence and structure alignment, they are classified into five different fold types [14], but significant common structural and functional elements have been shown to be shared by all PLP-dependent proteins [15]. The structural and functional similarities within and across the protein subgroups often exist with low sequence homologies, as in the case of tryptophan synthase (TS) and OASS, both belonging to the β-family and fold type II. This feature makes PLP-dependent enzymes ideal systems in which to investigate the delicate interplay between the primary sequence and the coenzyme-mediated effects in determining the folding mechanism, functional structure and global and local stability of the native conformation(s). The role of the coenzyme in folding mechanism and structural stabilization has been characterized only for a limited number of PLP-dependent proteins ([12] and references therein). The present experimental evidence does not indicate any correlation between the mechanisms of folding and stabilization and the functional families or structural types. A recent investigation of the guanidinium hydrochloride-induced unfolding of OASS [12] supports this view. In contrast to other

PLP-proteins, the coenzyme was found to affect qualitatively and quantitatively the native structure of OASS, and to confer a significant thermodynamic stabilization to the enzyme with respect to chemical denaturation [12]. The results also suggested that such stabilizing action might affect to a different extent the two domains that constitute each subunit of OASS. It has been proposed that the relatively low thermodynamic stability observed for many globular proteins [16], inhibitory serpins and some viral membrane fusion proteins [17] allows the plasticity necessary for protein activity. Since specialized regions within each macromolecule fulfill specific tasks in protein function and regulation, it is reasonable to assume that individual domains are endowed with different stability depending on the extent of conformational flexibility required for biological functions. Therefore, it is of considerable interest (i) to assess the relative thermodynamic stability of the N- and C-terminal domains of OASS and (ii) to relate it to the dynamics associated to protein function and regulation.
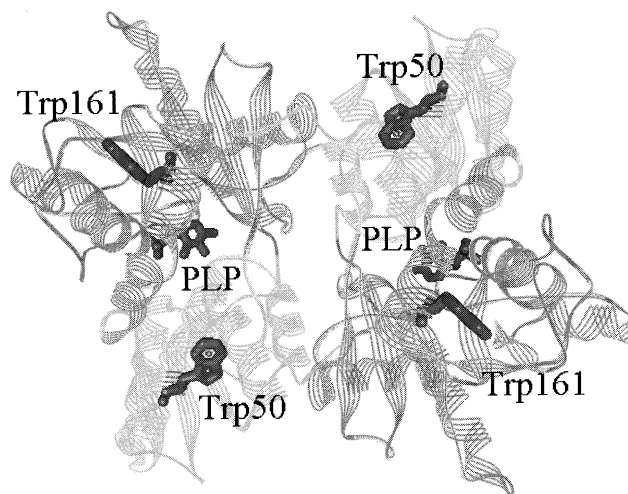

Fig. 1. Three-dimensional structure of *Salmonella typhimurium* holo-OASS dimer (PDB file 1OAS). Residues 1–12 and 35–145 constitute the N-terminal domain (light gray), while residues 13–34 and 146–315 belong to the C-terminal domain (dark gray) [1]. The coenzyme pyridoxal 5′-phosphate and the two tryptophan residues, Trp50 and Trp161, are shown in stick mode.

2. Materials and methods

2.1. Enzyme

The A-isozyme of *O*-acetylserine sulfhydrylase from *S. typhimurium*, prepared as previously described [18], was a kind gift of Dr. Paul F. Cook (Department of Chemistry and Biochemistry, University of Oklahoma, Norman, OK, USA). An extinction coefficient of 7600 M^{-1} cm^{-1} at 412 nm [19] was used to estimate holo-OASS concentration. The apo-enzyme was prepared by dialyzing holo-OASS first against a solution containing 5 M GdnHCl, 100 mM MES, 10 mM *O*-acetylserine, 0.1 mM dithiothreitol (pH 6.5) at 4°C, and then against 100 mM potassium phosphate, 0.1 mM dithiothreitol, pH 7.0 [20]. The concentration was determined by the Bradford method [21]. An extinction coefficient of 20 000 M^{-1} cm^{-1} at 280 nm was obtained for apo-OASS protomers using holo-OASS to build a calibration curve.

2.2. Chemicals

K^+ HEPES, MES, guanidium hydrochloride, *N*-acetyl-L-tryptophanamide, *O*-acetyl-L-serine, fluorescein (Sigma), dithiothreitol (Fluka) and *p*-terphenyl (Aldrich) were of the best commercially available quality and were used without further purification.

2.3. Buffers

Unless otherwise stated, all experiments were carried out in a buffer solution containing 100 mM K^+ HEPES (pH 7.0), and variable concentrations of GdnHCl, at 20°C. Denaturant-containing solutions were prepared according to Pace [22].

2.4. Time-resolved fluorescence measurements

Fluorescence intensity decays were measured by the phase and modulation technique [23,24].

Tryptophan fluorescence lifetimes of holo- and apo-OASS were measured at a protomer concentration of 9.65 and 4.80 μM, respectively, upon excitation at 295 nm. A *p*-terphenyl solution in ethanol (1.05 ns) was used as a lifetime standard reference. A frequency-doubled, cavity-dumped rhodamine dye laser (Coherent, Model 700), synchronously pumped by a Coherent Antares Nd/YAG laser, was used as a source of the modulated light. In order to eliminate scattering of the excitation light by the sample, fluorescence emission was collected through a long-pass filter (Schott WG320).

The fluorescence lifetimes of the internal aldimine Schiff base, upon excitation at 454.5 nm, were measured at a holo-enzyme concentration of 19.3 μM (protomers). A fluorescein solution in diluted NaOH was used as a lifetime standard reference (4.05 ns). The modulated excitation light was obtained using an argon–ion laser (Spectra Physics, Model 2017) modulated through a Pockel cell. The emission was collected through a Hoya Y48 long-pass filter.

To eliminate polarization artifacts in the intensity decay, data were collected under magic angle conditions with the excitation light polarized normal to the laboratory plane, 0°, and the emission polarizer oriented at 54.7° [25]. Samples were equilibrated at 20 ± 0.5°C using a jacketed cell holder and a circulating water bath. Since the unfolding rate of OASS is of the order of hours at low denaturant concentration [12], each sample was pre-incubated at the final GdnHCl concentration for at least 24 h, at 20°C. The data were fitted to a sum of discrete exponentials [26] with lifetime τ_i and fractional intensity f_i by the Marquardt algorithm of the Globals Unlimited software (University of Illinois, Urbana, IL, USA) [27]. Frequency-independent standard errors of 0.2°, for phase data, and 0.004, for modulation data, were routinely applied. The chi-square (χ^2) minimization was the criterion used to select the best fits [28,29]. The mean lifetimes $\langle \tau \rangle$ were obtained from the calculated lifetimes τ_i and fractional intensities f_i according to the equation [30]

$$\langle \tau \rangle = \sum \alpha_i \cdot \tau_i \tag{1}$$

where α_i, the pre-exponential factor for a multi-exponential decay law, was determined by Eq. 2

$$\alpha_i = \frac{\dfrac{f_i}{\tau_i}}{\sum \dfrac{f_i}{\tau_i}} \tag{2}$$

2.5. Equilibrium denaturation curves

For all considered signals (τ_i, $\langle\tau\rangle$ or circular dichroism at 222 nm) the dependence of signal intensity I on denaturant concentration $[D]$ was fitted to a two-state model according to equation

$$I = \frac{I_N + (I_U + S_U[D])e^{\dfrac{([D]-D_{50})m}{RT}}}{1 + e^{\dfrac{([D]-D_{50})m}{RT}}} \qquad (3)$$

where I_N and I_U are the extrapolated signal values for the fully native and denatured protein, respectively, S_U a post-transitional slope reflecting the denaturant dependence of the signal, D_{50} the denaturant concentration at half transition and m the denaturant index. The experimental data points were then converted to fraction of total effect F_U by using the fitting parameters previously determined, according to the equation

$$F_U = \frac{I_N - I}{I_N - (I_U + S_U[D])} \qquad (4)$$

Finally, the dependence of the fraction of total effect F_U on denaturant concentration $[D]$ was analyzed according to the equation

$$F_U = \frac{e^{\dfrac{([D]-D_{50})m}{RT}}}{1 + e^{\dfrac{([D]-D_{50})m}{RT}}} \qquad (5)$$

3. Results and discussion

3.1. Coenzyme fluorescence

The coenzyme fluorescence intensity decays, upon excitation at 454.5 nm, are well described by two discrete exponentials (Fig. 2). On the basis of previous studies on native holo-OASS [10], the long (Fig. 2, circles) and short-lived components (Fig. 2, squares) have been attributed to the ketoenamine tautomer of the internal aldimine and to a dipolar species occurring upon imine proton dissociation in the excited state, respectively. The fractions of the two components are GdnHCl-independent, while

the lifetimes are slightly affected by the denaturant concentration (Fig. 2). The total fluorescence intensity upon coenzyme fluorescence excitation at 454.5 nm drops sharply with the increase of GdnHCl concentration, and reliable measurements could not be carried out above 2.0 M. These results are in agreement with absorption and ^{31}P nuclear magnetic resonance data [12] and indicate that most of the coenzyme is released from the protein upon exposure to 2.0 M GdnHCl. Therefore, coenzyme fluorescence only probes the active site conformation of the fraction of protein molecules with bound PLP and cannot be considered a valuable probe to monitor the global unfolding process.
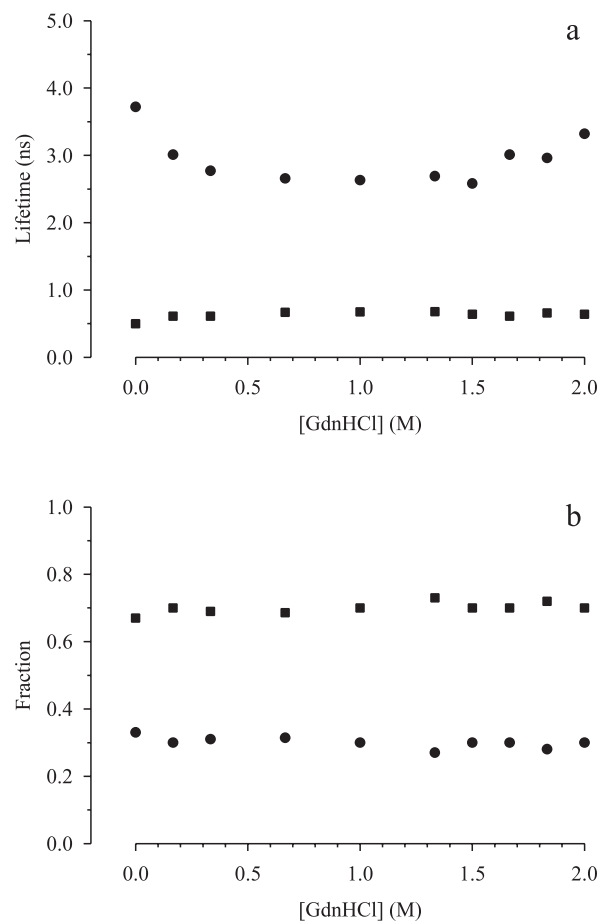

Fig. 2. Dependence of PLP fluorescence lifetimes (a) and relative fractional intensities (b) on GdnHCl concentration, upon excitation at 454.5 nm. Experiments were carried out on a solution containing 19.3 μm holo-OASS, 100 mM HEPES (pH 7) at 20°C, after equilibration for 24 h at the desired GdnHCl concentration. Each point is the best fit to 2–4 separate experiments. Data sets with global χ^2 value higher than 1.2 were discarded.

3.2. Tryptophan lifetimes assignment and protein stability

Triple-exponential decay models were required to adequately fit tryptophan fluorescence decays of the holo- and the apo-enzyme (Figs. 3 and 4). In native conditions a long-lived component ($\tau \cong 5.5$ ns) (Figs. 3 and 4, open circles), significantly populated in the apo-enzyme ($f = 0.481$), is strongly quenched in the holo-enzyme ($f = 0.055$). This different behavior of holo and apo-OASS in the absence of denaturant is
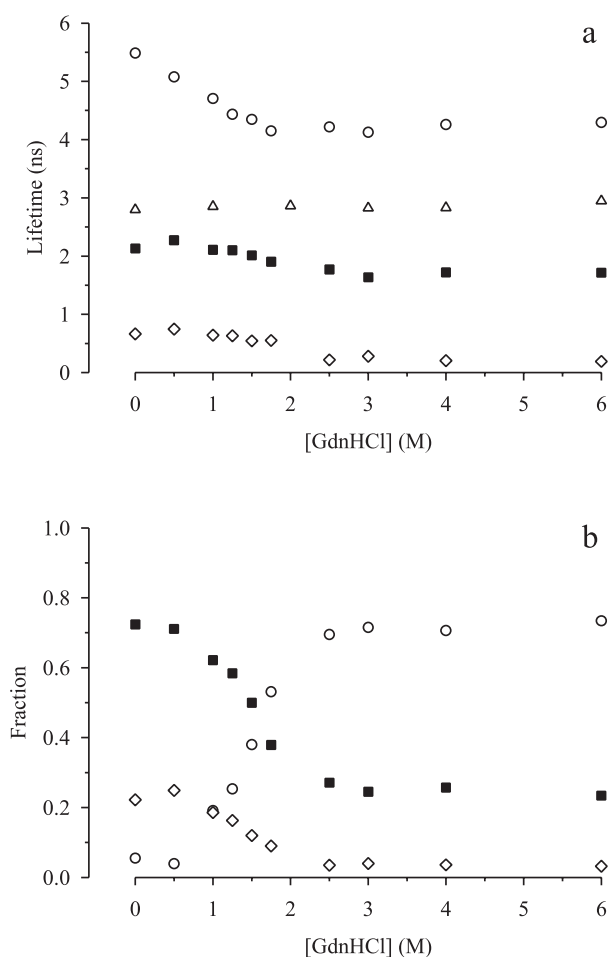

Fig. 3. Trp fluorescence lifetimes of holo-OASS as a function of GdnHCl concentration, upon excitation at 295 nm. The lifetimes (a) and the corresponding fractional intensities (b) were measured for solutions containing 9.65 μM protomers, 100 mM HEPES (pH 7) at 20°C. Each sample was equilibrated for 24 h at the desired GdnHCl concentration, at 20°C. Each point is the best fit to 2–7 separate experiments. All reported data have global $\chi^2 < 1.0$. For comparison, the single emission lifetime of NATA is reported in panel a ($\triangle$).
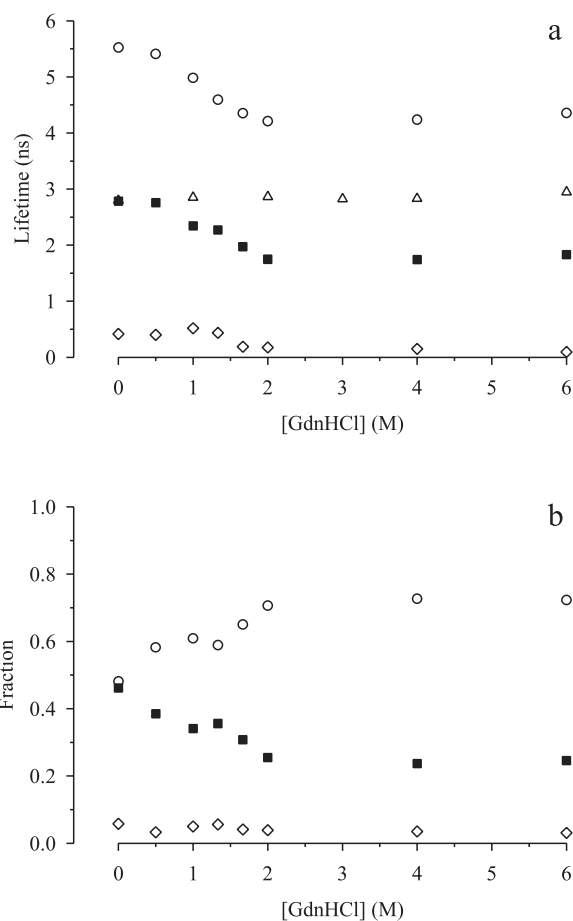

Fig. 4. Trp fluorescence lifetimes of apo-OASS as a function of GdnHCl concentration, upon excitation at 295 nm. The lifetimes (a) and the corresponding fractional intensities (b) were measured for solutions containing 4.80 μM protomers, 100 mM HEPES (pH 7) at 20°C. Each sample was equilibrated for 24 h at the desired GdnHCl concentration, at 20°C. Each point is the best fit to 2–7 separate experiments. All reported data have global $\chi^2 < 1.0$. For comparison, the single emission lifetime of NATA is reported in panel a ($\triangle$).

due to conformational changes upon binding of the coenzyme, affecting the secondary structure of the enzyme [12], and the Forster energy transfer occurring from Trp50 to the PLP [8,11]. Both of these phenomena influence the relative contribution of the two tryptophan residues to the emission of the holo- and the apo-enzyme. An intermediate component ($\tau \cong 2.5$ ns) (Figs. 3 and 4, closed squares), predominant in the native holo-OASS, likely arises from the contribution of both tryptophans. A fast component is also present (Figs. 3 and 4, open diamonds), with a fractional intensity of about 22% and 5.8% for native holo- and apo-OASS, respectively.

The denaturant concentration dependence of fluorescence lifetimes and fractional intensities (Figs. 3 and 4) indicates that the unfolding of both holo- and apo-OASS, as monitored by tryptophan fluorescence, is complete at about 2 M GdnHCl. Upon unfolding, different events affect Trp emission: a partial loss of secondary and tertiary structure, a higher exposure to the solvent, and the abolishment of the energy transfer to the PLP. At high denaturant concentrations (≥ 2.5 M) the behavior of holo- and apo-protein is no longer distinguishable and no additional effects are observed by further increasing denaturant concentrations. The slight, linear dependence of lifetimes and fractions on GdnHCl concentration (Figs. 3 and 4) simply reflects the denaturant-dependent changes of Trp emission, as shown by the comparison with NATA lifetimes (Figs. 3 and 4).

The emission decay data of the denatured holo- and apo-enzyme show heterogeneity and cannot be fit to a single exponential decay model, in contrast to the model compound NATA (Figs. 3 and 4). Accordingly, the Trp emission spectra never match those collected on NATA under comparable conditions (data not shown). As also indicated by the far-UV circular dichroism spectra and the fluorescence anisotropy decays [12], this result suggests that even under strongly denaturing conditions the Trp-containing regions still retain some structural organization.

The equilibrium unfolding curves for holo-OASS, as monitored by far-UV circular dichroism and by tryptophan mean fluorescence lifetimes $\langle \tau \rangle$, are shown in Fig. 5a. The mean fluorescence lifetimes have been calculated from the three individual lifetimes τ_i and fractional intensities f_i (Fig. 3) as indicated in Section 2 (Eqs. 1 and 2). The midpoint for the denaturant dependence of the mean lifetimes is 1.45 ± 0.04 M GdnHCl, in good agreement with the value of 1.57 ± 0.15 M previously reported for steady state fluorescence upon excitation at 298 nm [12]. The observed transition midpoint is significantly higher than that of 1.02 ± 0.01 M obtained from the far-UV circular dichroism data (Fig. 5a). Since far-UV circular dichroism probes the average secondary structure content of the protein and fluorescence is sensitive to the local environment of the fluorophores, these results indicate that one or both tryptophans are located in regions endowed with
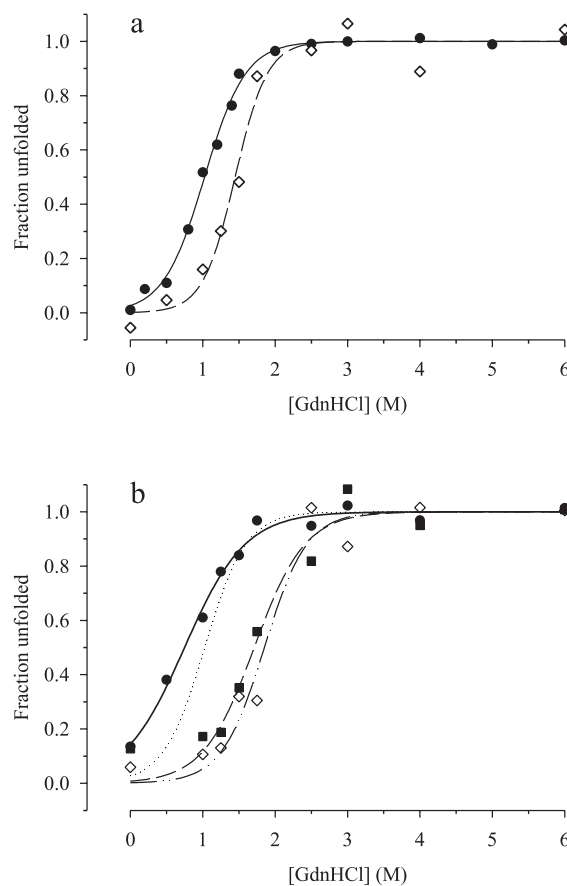

Fig. 5. (a) Equilibrium denaturation curves of holo-OASS, as monitored by circular dichroism at 222 nm (●) and mean fluorescence lifetime upon excitation at 295 nm (◇). Circular dichroism data are from the experiments reported by Bettati et al. [12]. The mean fluorescence lifetime was calculated according to Eq. 1. In both cases the experimental data points were fitted to a two-state equilibrium denaturation curve according to Eq. 3 (data not shown). Fractions of total effect were calculated according to Eq. 4. The curves through data points are the best fit to Eq. 5. (b) Denaturant concentration dependence of holo-OASS tryptophan fluorescence lifetimes, upon excitation at 295 nm. Symbols are the same as in Fig. 3 for the longer (○), intermediate (■) and shorter (◇) lifetime. Fractions of total effect were calculated as reported in panel a. The curves through data points are the best fit to Eq. 5. The calculated equilibrium denaturation curve as monitored by circular dichroism at 222 nm (panel a) is reported for comparison (dotted line). For experimental conditions see legend to Fig. 3.

high stability, when compared to the average behavior of holo-OASS.

3.3. Differential domains stability

Trp50 and Trp161 belong to the N- and C-terminal domain of OASS, respectively. Despite the fact that the active site is located at the interface between the two domains, it has been suggested [12] that different interactions of the cofactor with residues belonging to the two domains could account for a stronger stabilizing effect on the C-terminal domain. Since an energy transfer predominantly occurs from Trp50 to PLP (in the native enzyme), we took advantage of the different contribution of Trp50 and Trp161 to the total emission and microscopic lifetimes of holo-OASS to resolve the differential stability of N- and C-terminal domains. In the absence of denaturant, the fluorescence emission of Trp50 is strongly quenched by energy transfer to the coenzyme [11]. Thus, Trp161 dominates the fluorescence emission of native holo-OASS. The contribution of Trp50 to the fluorescence emission of apo-OASS is not quenched by energy transfer to the coenzyme. Accordingly, the time-resolved fluorescence data for native holo- and apo-OASS (Figs. 3 and 4) exhibit a striking difference in the distribution of fluorescent species. In the apo-OASS the fractional intensity of the long-lived component ($\tau \cong 5.5$ ns) is comparable to that of the species with intermediate lifetime (Fig. 4). In the holo-OASS (Fig. 3), the fractional intensity of the long-lived species is much lower ($f \cong 5\%$), suggesting that this lifetime component can be attributed to the fluorescent species quenched through energy transfer. This connection is strengthened by the behavior of the observed lifetimes upon protein unfolding. Concurrent with the abolishment of energy transfer in holo-OASS, the fractional contribution of long-lived components to the total emission increases, eventually matching that observed for apo-OASS (Figs. 3 and 4). Thus, it is reasonable to assume that the fluorescence emission by Trp50 affects the long-lived component detected by time-resolved fluorescence ($\tau_1 \cong 5.5$ ns) at a higher extent with respect to the intermediate ($\tau_2 \cong 2.5$ ns) and fast component. The low population of τ_1 in native holo-OASS rules out a significant contribution to this species by Trp161 emission, which is not quenched

through energy transfer to PLP. As a consequence, the comparison of the denaturant dependence of τ_1 and τ_2 can be used to analyze, at least qualitatively, the differential stability of the N- and C-terminal domains of OASS. Fig. 5b shows the dependence on denaturant concentration of the three lifetimes calculated from the fitting of holo-OASS time-resolved fluorescence data. The midpoint of the unfolding transition as monitored by τ_1 (0.75 ± 0.03 M GdnHCl) is significantly lower with respect to those calculated for τ_2 and τ_3 (1.71 ± 0.09 and 1.85 ± 0.09, respectively). The former midpoint is even lower than that observed for the far-UV circular dichroism, while the others are slightly higher than those observed with steady-state fluorescence. Overall, these results indicate that Trp50 is located in a protein region (N-terminal domain) endowed with significantly lower stability with respect to that containing Trp161 (C-terminal domain). This behavior is not associated to the different sequence and conformation of the two domains, since the unfolding of apo-OASS is characterized by the overlapping of the unfolding curves obtained with non-correlated probes [12]. Significantly, structural data indicate that the N- and C-terminal domains of OASS are characterized by a high degree of structural homology [1], as also observed in tryptophan synthase and several multidomain proteins ([31] and references therein). Therefore, the experimental evidence points to a differential stabilizing effect elicited by the coenzyme via the interactions with the two domains [12]. These include a network of hydrogen bonds between the phosphate group of the coenzyme, the N-terminus of helix 7 and several residues (176–178, 180) of the C-terminal domain [1]. This differential stability could have an important functional role for the protein. It has been reported [2] that the formation of the external aldimine of holo-OASS is accompanied by the movement of a subdomain (residues 87–131) belonging to the N-terminal domain of the enzyme. This conformational change implies a large structural plasticity and is likely to require a low thermodynamic stability.

References

[1] P. Burkhard, G.S.J. Rao, E. Hohenester, K.D. Schnackerz, P.F. Cook, J.N. Jansonius, J. Mol. Biol. 283 (1998) 121–133.

[2] P. Burkhard, C.-H. Tai, C.M. Ristroph, P.F. Cook, J.N. Jansonius, J. Mol. Biol. 291 (1999) 941–953.

[3] P. Burkhard, C.-H. Tai, J.N. Jansonius, P.F. Cook, J. Mol. Biol. 303 (2000) 279–286.

[4] A. Mozzarelli, S. Bettati, A.M. Pucci, P. Burkhard, P.F. Cook, J. Mol. Biol. 283 (1998) 135–146.

[5] V.D. Rege, N.M. Kredich, C.-H. Tai, W.E. Karsten, K.D. Schnackerz, P.F. Cook, Biochemistry 35 (1996) 13485–13493.

[6] G.D. McClure, P.F. Cook, Biochemistry 33 (1994) 1674–1683.

[7] K.D. Schnackerz, C.-H. Tai, J.W. Simmons, T.M. Jacobson III, G.S.J. Rao, P.F. Cook, Biochemistry 34 (1995) 12152–12160.

[8] G.B. Strambini, P. Cioni, P.F. Cook, Biochemistry 35 (1996) 8392–8400.

[9] S. Benci, S. Vaccari, A. Mozzarelli, P.F. Cook, Biochemistry 36 (1997) 15419–15427.

[10] S. Benci, S. Vaccari, A. Mozzarelli, P.F. Cook, Biochim. Biophys. Acta 1429 (1999) 317–330.

[11] S. Benci, S. Bettati, S. Vaccari, G. Schianchi, A. Mozzarelli, P.F. Cook, J. Photochem. Photobiol. B 48 (1999) 17–26.

[12] S. Bettati, S. Benci, B. Campanini, S. Raboni, G. Chirico, S. Beretta, K.D. Schnackerz, T.L. Hazlett, E. Gratton, A. Mozzarelli, J. Biol. Chem. 275 (2000) 40244–40251.

[13] F.W. Alexander, E. Sandmeier, P.K. Mehta, P. Christen, Eur. J. Biochem. 219 (1994) 953–960.

[14] N.V. Grishin, M.A. Phillips, E.J. Goldsmith, Protein Sci. 4 (1995) 1291–1304.

[15] K.A. Denessiouk, A.I. Denesyuk, J.V. Lehtonen, T. Korpela, M.S. Johnson, Proteins 35 (1999) 250–261.

[16] R. Jaenicke, Biochemistry 30 (1991) 3147–3161.

[17] C. Lee, S.-H. Park, M.-Y. Lee, M.-H. Yu, Proc. Natl. Acad. Sci. USA 97 (2000) 7727–7731.

[18] C.-H. Tai, S.R. Nalabolu, T.M. Jacobson, D.E. Minter, P.F. Cook, Biochemistry 32 (1993) 6433–6442.

[19] M.A. Becker, N.M. Kredich, G.M. Tomkins, J. Biol. Chem. 244 (1969) 2418–2427.

[20] K.D. Schnackerz, P.F. Cook, Arch. Biochem. Biophys. 324 (1995) 71–77.

[21] M. Bradford, Anal. Biochem. 72 (1976) 248–254.

[22] C.N. Pace, Methods Enzymol. 131 (1986) 266–280.

[23] R.D. Spencer, G. Weber, Ann. N.Y. Acad. Sci. 158 (1969) 361–376.

[24] E. Gratton, M. Limkeman, Biophys. J. 44 (1983) 315–324.

[25] R.D. Spencer, G. Weber, J. Chem. Phys. 52 (1970) 1654–1663.

[26] D.M. Jameson, E. Gratton, R.D. Hall, Appl. Spectrosc. Rev. 20 (1984) 55–105.

[27] J.M. Beechem, E. Gratton, SPIE 909 (1988) 70–81.

[28] E. Gratton, D.M. Jameson, L.D. Hall, Annu. Rev. Biophys. Bioeng. 13 (1984) 105–124.

[29] R.M. Jameson, T.L. Hazlett, in: D.G. Dewey (Ed.), Biophysical and Biochemical Aspects of Fluorescence Spectroscopy, Plenum Press, New York, 1991, pp. 105–133.

[30] M.R. Eftink, Biophys. J. 66 (1994) 482–501.

[31] C.C. Hyde, S.A. Ahmed, E.A. Padlan, E.W. Miles, D.R. Davies, J. Biol. Chem. 263 (1988) 17857–17871.